Ocean stratification impedes particulate transport to the plumes of Enceladus

Article

Supplemental Material

It is advisable to refer to the publisher's version if you intend to cite from the work. See Guidance on citing.

To link to this article DOI: http://dx.doi.org/10.1038/s43247-025-02036-3

www.reading.ac.uk/centaur

CentAUR

Central Archive at the University of Reading

Supplementary material

Parameter	Value
Ice shell surface radius (r_{s})	252 km
Core radius (r_{c})	192 km
Ocean thickness (H_{o})	40 km
Ice thickness (H_{i})	20 km
Ice density (ρ_{i})	925 kg m^{-3}
Gravity at ice shell surface (g)	0.113 m s^{-2}
Ocean mean salinity (S_{ref})	5, 10, 15, 17.5, 20, 22.5 g kg^{-1}
Ocean reference pressure (P_{ref})	$\rho_{\mathrm{i}} \int_{H_{\mathrm{i}}}^{0} g(z)\, dz$
Ocean reference temperature (T_{ref})	Freezing temp at P_{ref} and S_{ref}
Ocean reference density (ρ_0)	Density at T_{ref}, P_{ref} and S_{ref}
Core density (ρ_{core})	2370 kg m^{-3}
Rotation rate (Ω)	5.307 x 10^{-5} s^{-1}
Core total heat output (F_{tot})	20 GW
Specific heat capacity (c_p)	4000 J kg^{-1} K^{-1}
Eddy diffusivity (κ_{GM})	1 m^2 s^{-1}
Vertical diffusivity (κ_z)	10^{-5}, 10^{-4}, 10^{-3} m^2 s^{-1}
Prandtl number ($\frac{\nu}{\kappa}$)	10
Ice melting viscosity (η_{melt})	10^{-14} Pa s

Table S1: Key parameters used in default numerical simulations and in computation of boundary forcings.
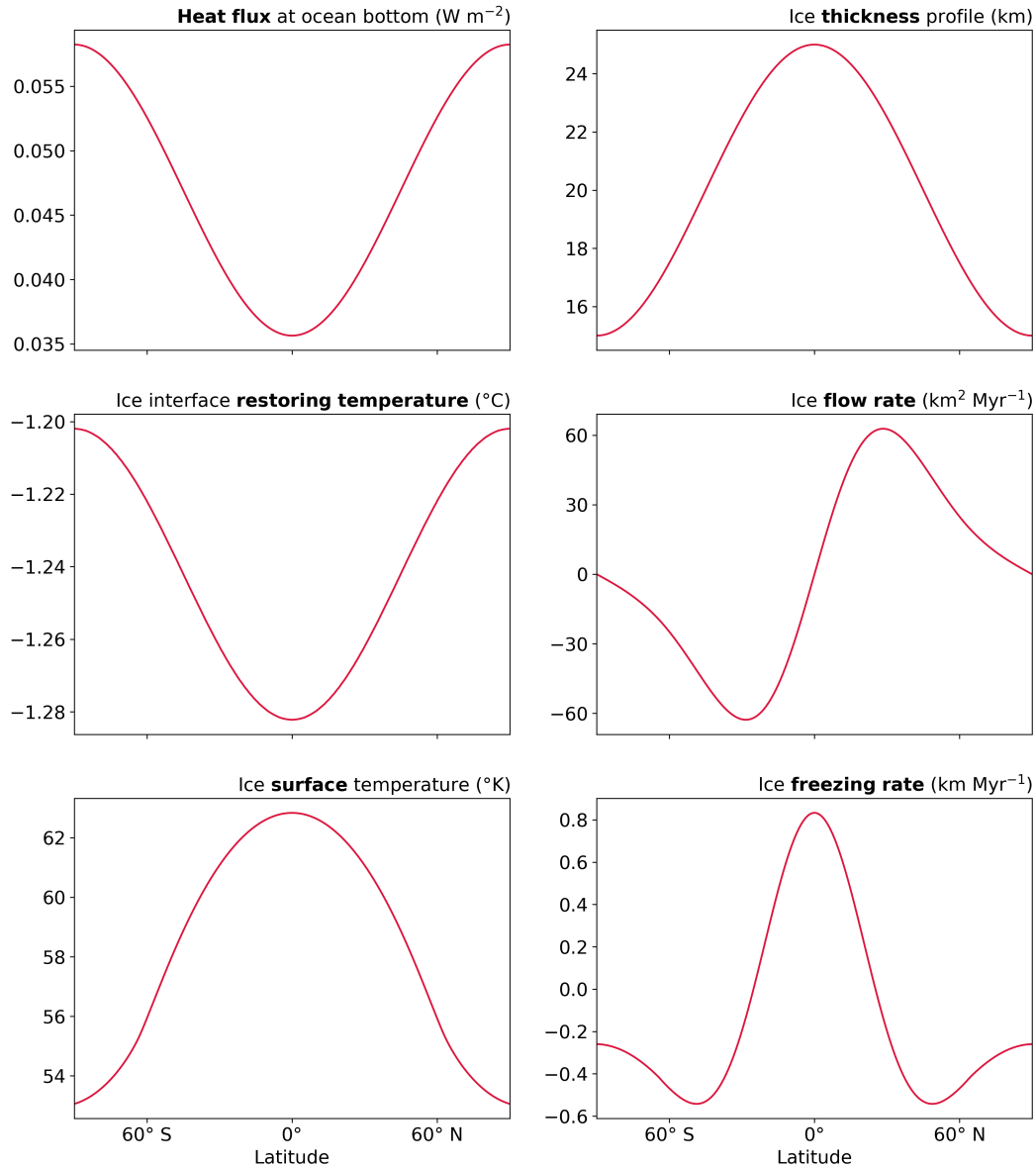
Figure S1: **Top Left**: Bottom heating profile used in simulations (W m^{-2}), assuming a total global core heat output of 20 GW. **Middle left**: An example restoring temperature (^{o}C) profile at the ocean top (ice-interface) used in simulations at 20 g kg^{-1} - corresponding to the pressure and salinity dependant freezing temperature. **Bottom left**: Surface temperature (^{o}K) of ice used to compute ice flow rate in middle right panel. **Top right**: Idealised ice thickness profile (km) used to compute the ice-interface restoring temperature and ice flow rate (for use in computation of ice freezing rate). Note the topography itself is not used in simulations, which assume a flat ocean top. **Middle right**: Ice flow rate (km^2 per million years) used for computing the freshwater flux at the ocean top, in turn computed from the idealised geometry of the top right panel, assuming a steady state Enceladus ice shell thickness profile. **Bottom right**: Freshwater flux (km per million years) profile applied at the ocean top in simulations, computed using the ice flow rate in the middle right panel.

3
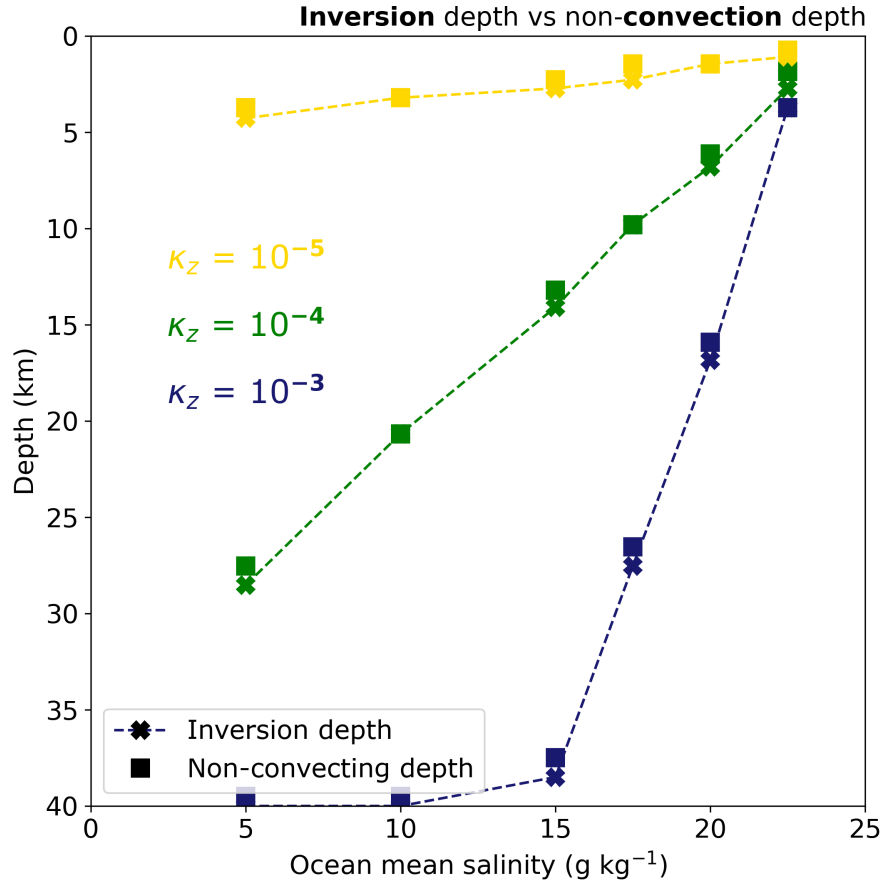
Figure S2: Numerical solution for the inversion depth (km - cross, dashed line - depth at which the thermal expansion coefficient α_T becomes negative) across a range of ocean mean salinity (g kg^{-1}) for three values of κ_z (m^2 s^{-1}), denoted with different colours, as in Fig. 2 of the main text. Here the inversion depth is plotted alongside the depth at which model convection extending from the ocean bottom stops (km - squares), defined as the depth at which the laterally-averaged convecting time falls below 0.01% of model time. Markers at 40 km depth denote where there is no inversion depth (meaning α_T remained negative across the whole ocean) or non-convecting depth (meaning no convection extended from the ocean bottom) respectively.
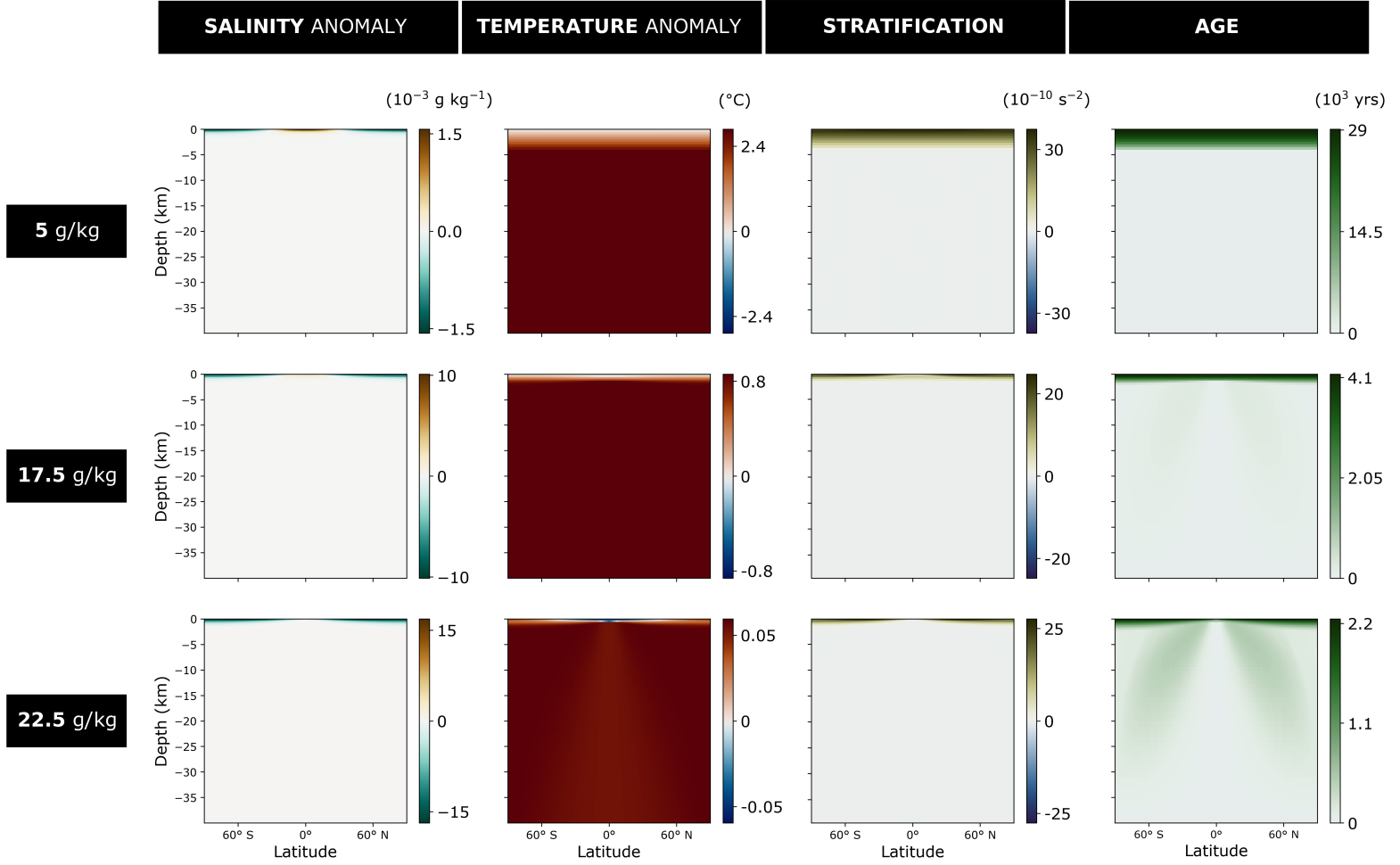
Figure S3: Numerical solutions with effective vertical diffusivity $\kappa_z = 10^{-5}$ m^2 s^{-1}, across three different mean ocean salinities of 5 (top), 17.5 (middle), and 22.5 (bottom) g kg^{-1}, highlighting stratification regimes at a lower κ_z than presented in the main text. Note colour bar scales are saturated and vary throughout. **First column**: Salinity anomaly (g kg^{-1}) taken about the mean salinity. **Second column**: Potential temperature anomaly ($^\circ$ C) taken about the simulation reference temperature T_{ref} (freezing temperature computed under 20 km mean ice thickness) of -0.433 (top), -1.106 (middle) and -1.379 (bottom) $^\circ$ C. **Third column**: Buoyancy frequency N^2 (s^{-2}) indicating stratification. **Fourth column**: Ideal age of tracers (years), sourced from the ocean bottom.
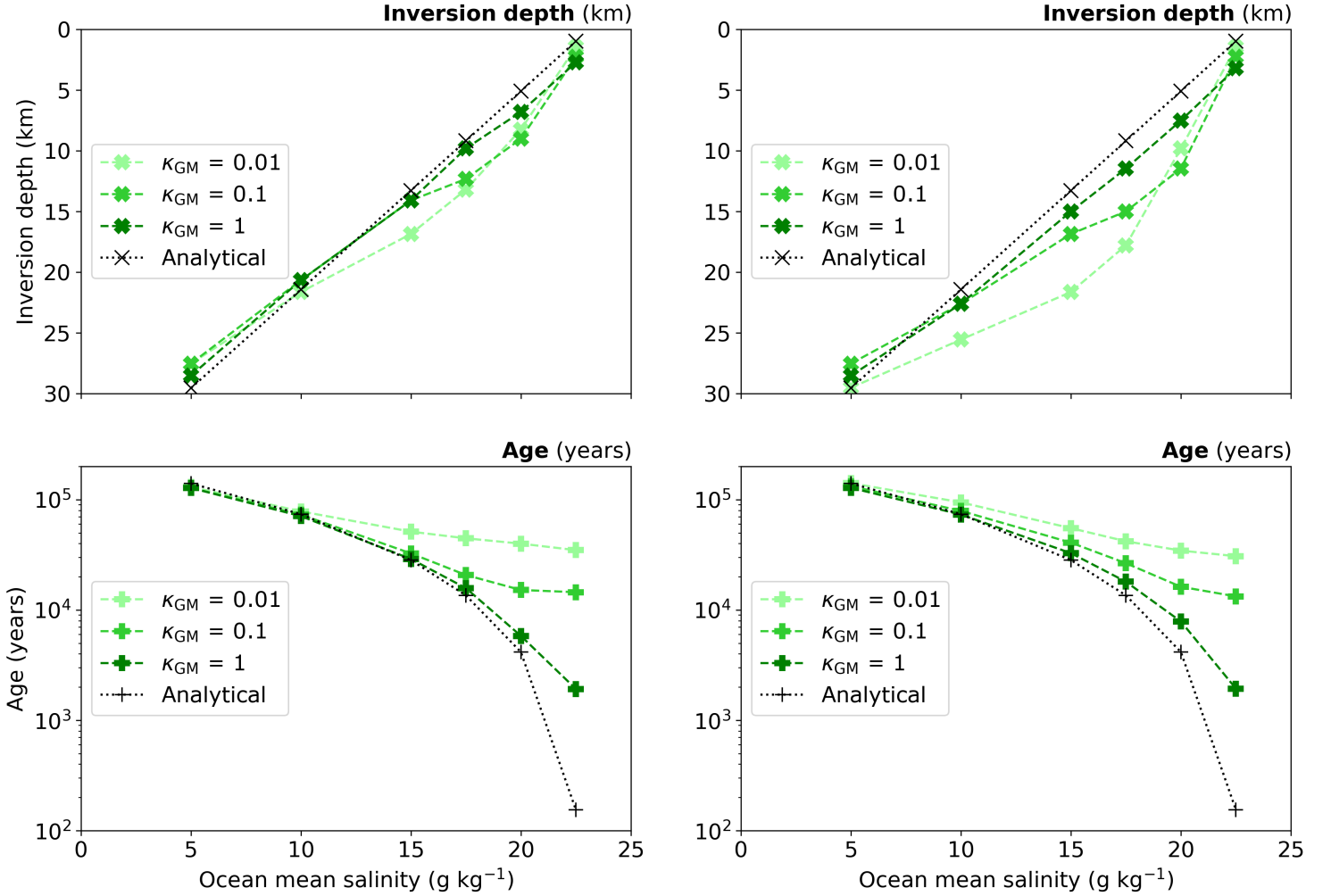
Figure S4: **Top**: Numerical solution for the inversion depth (km - depth at which the thermal expansion coefficient α_T becomes negative), as in Fig. 2 of the main text across a range of ocean mean salinity (g kg^{-1}), but plotted for three different values eddy diffusivity κ_{GM} (m^2 s^{-1}), indicated with varying shade of green, for constant vertical diffusivity $\kappa_z = 10^{-4}$ m^2 s^{-1}. The analytical solution (black) using Eq. (5) is plotted alongside for comparison. **Bottom**: Corresponding numerical solution for the ideal age at the south polar ocean-ice interface, plotted alongside the analytical solution (Eq. (6)). **Left**: Solutions at a melting viscosity $\eta_{\mathrm{melt}} = 10^{-14}$ Pa s as used in default simulations of the main paper. **Right**: solutions with $\eta_{\mathrm{melt}} = 2\mathrm{x}10^{-13}$ Pa s, which creates a 5 times larger magnitude of ice melting and freezing at the ocean top. Note increasing discrepancies relative to analytical solution at higher salinity and lower κ_{GM}, due to the formation of freshwater lenses at the ocean-ice interface at the poles.
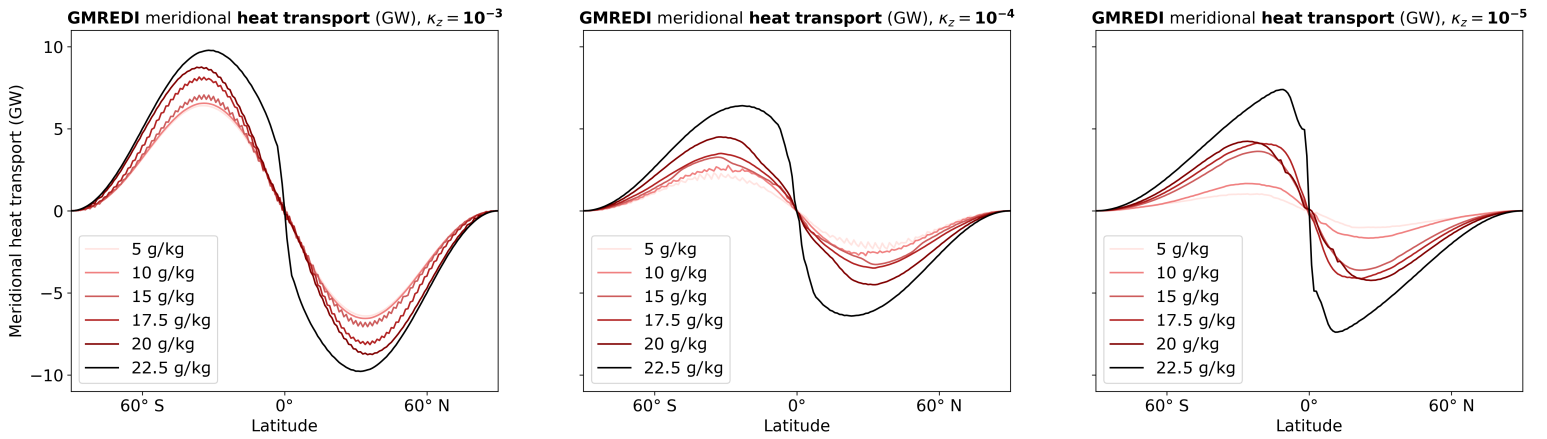
Figure S5: Vertically-integrated global meridional heat transport (GW) achieved by parameterised eddies (GMREDI) in numerical solutions. Plotted across modelled ocean mean salinity at a modelled effective vertical diffusivity κ_z of 10^{-3} (left), 10^{-4} (middle), and 10^{-5} (right) m^2 s^{-1}. The eddy diffusivity $\kappa_{\mathrm{GM}} = 1$ m^2 s^{-1} for the presented solutions. Note the heat transports shown here are scaled up by a factor 360 to be representative of the global ocean (as the 2D simulations are based on a 1 degree wide single box in the zonal direction).
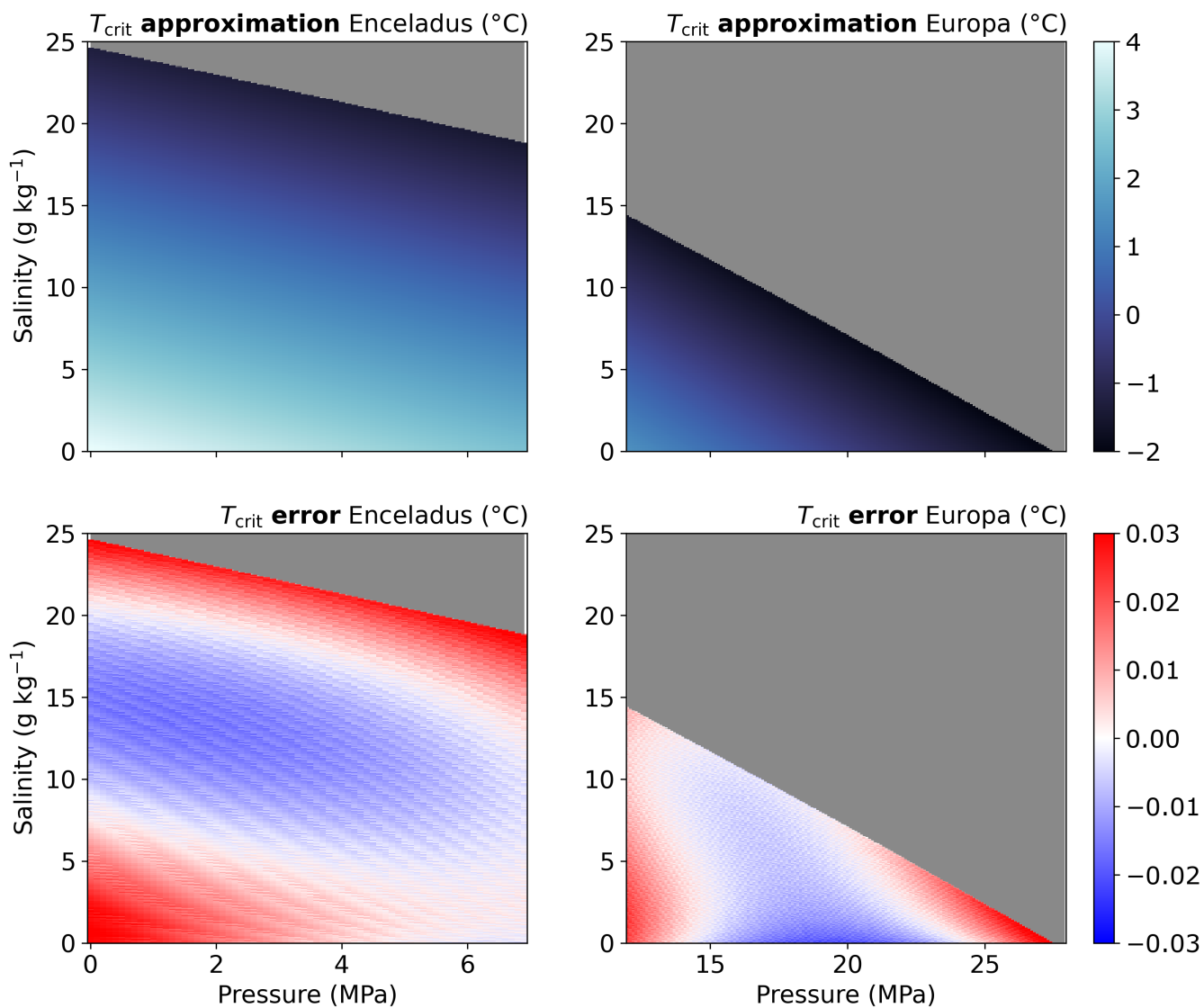
Figure S6: **Top:** Linearly approximated critical temperature (T_{crit} - ^{o}C) - defining the temperature at which the thermal expansion coefficient (α_T) changes sign - as a function of pressures (MPa) and salinity (g kg^{-1}) plausible for Enceladus (left) and Europa (right) respectively. Grey shading denotes where T_{crit} does not apply because α_T cannot become negative for the given salinity and pressure.

Bottom: Error of linear approximation of critical temperature (^{o}C) relative to reference computation described in the main text.
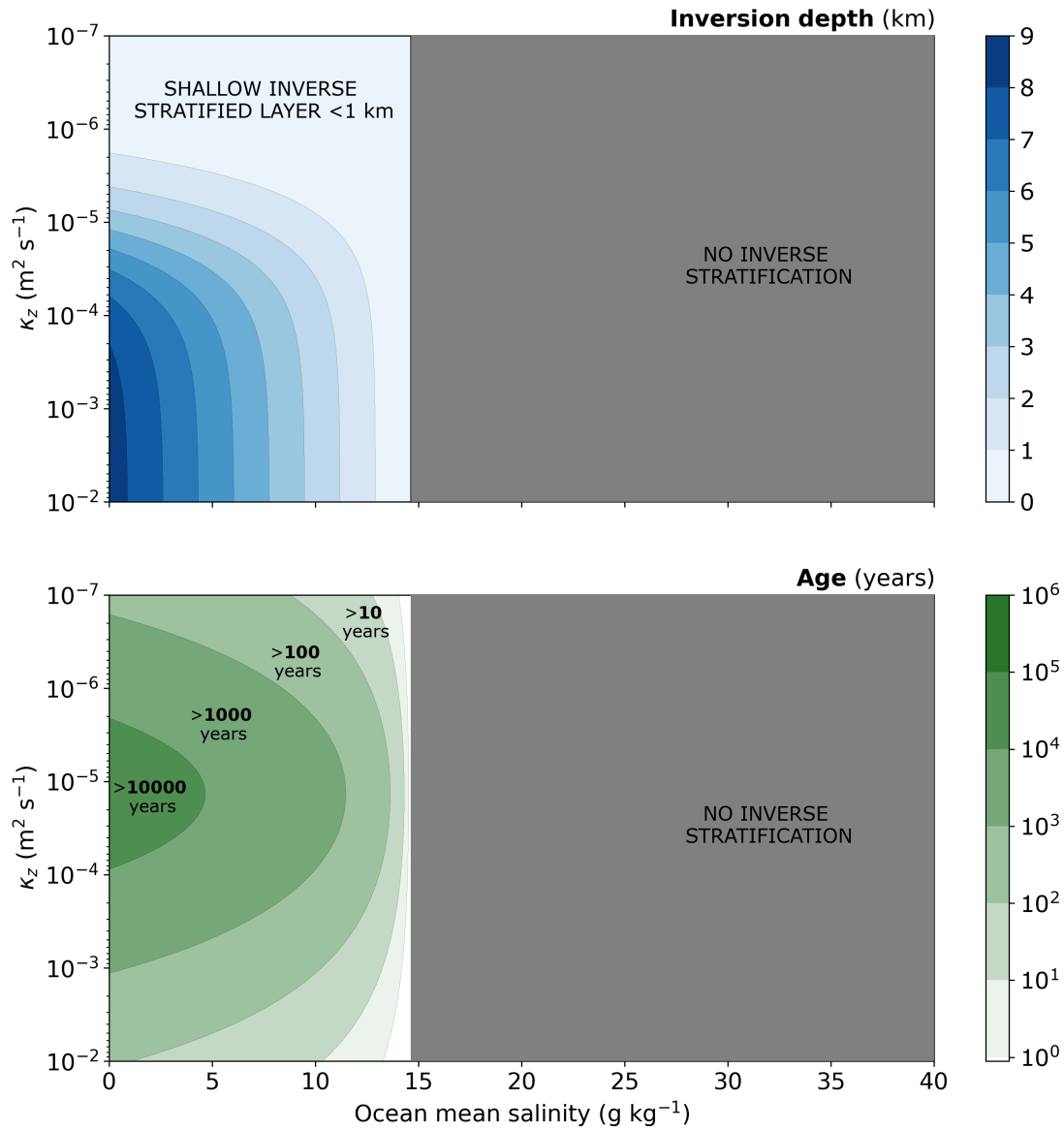
Figure S7: **Top**: Inversion depth H_{strat} (km - depth at which thermal expansion coefficient α_T becomes negative, taken here to define the inverse layer thickness) plotted as a function of ocean mean salinity (g kg^{-1}) and vertical diffusivity κ_z (m^2 s^{-1}), for Europa - moon of Jupiter. Grey shading denotes where inverse stratification cannot occur, because α_T cannot become negative at the ocean-ice interface pressure (computed under an assumed 10 km ice thickness). **Bottom**: Tracer age (years) at Europa's ocean-ice interface, computed using the theoretical model outlined in the main text. Note that age contours are logarithmic.